Egypt. J. Chem. **Vol. 65,** No. 12 pp. 21 - 26 (2022)

Egyptian Journal of Chemistry

http://ejchem.journals.ekb.eg/

Visualization the crystal structure, microstructure, magnetic performance and antimicrobial as well as anticancer activities of $La_{0.5}Sr_{0.5}Mn_{0.9}Ti_{0.1}O_3$ nanopowders

Hesham A. Hassan[1]*, Ali Omar Turky[2], Ali M. Hassan[1], Hosni A Gomaa[1] and Mohmed M. Rashad[2]

[1]*Chemistry Department, Faculty of Science, Al-Azhar University, Nasr City 11884, Egypt*

[2]*Electronic and Magnetic Materials Department, Advanced Materials Institute, Central Metallurgical Research & Development Institute, Helwan 87, Egypt*

Abstract

Titanium substituted lanthanum strontium manganite LSMTO ($La_{0.5}Sr_{0.5}Mn_{1-x}Ti_xO_3$, x= 0, 0.1) nanopowders were prepared via organic acid precursor using glycine-nitrate as fuel. The structural, microstructure, magnetic properties, anti-microbial activity as well as anti-cancer activity of $La_{0.5}Sr_{0.5}Mn_{0.9}Ti_{0.1}O_3$ at different calcination temperatures from 800 to 1200oC for 2h were scrutinized. The ideal orthorhombic perovskite LSMTO with a space group Pbnm was proved at different synthesis conditions. However, substitution of Ti^{4+} ion instead of Mn^{4+} ion in LSMO annealed at different temperatures led to an increment of the crystallite size from 13.57 to 16.10 nm. The FT-IR spectrum elucidated that the bands around 600 cm^{-1} associated with Mn-O turn out broad imputed to Ti-O stretching modes. The morphology of the produced samples appeared as spherical groupings. The temperature dependence of magnetization confirms that Ti^{+4} ions were weakness the ferromagnetic (FM)-paramagnetic (PM) double exchange transition as the result of the break in the FM Mn^{3+}–O–Mn^{4+} interactions. Molar magnetic susceptibility was notified to increase with the temperature. Subsequently, Curie temperature values were found to increase from 373 to 383 K with increasing the temperature, respectively. Eventually, LSMTO powders have cytotoxic effect on HepG-2 with IC_{50} value (105, 135 and 152 µg/ml) for LSMTO annealed at 800, 1000 and 1200 °C, respectively.

Keywords: Lanthanum strontium manganite, Fabrication, Characterization, Magnetic properties, Biomedical applications

1. Introduction

Lanthanum manganese oxide ($LaMnO_3$) is an A-type antiferromagnetic insulator where in manganese is present in Mn^{+3} state, by replacing La^{3+} with a divalent atom $LaMnO_3$ turn into ferromagnetic state because of divalent atom motivate a mixed-valence state of Mn ions (Mn^{+3}/Mn^{+4}). Lanthanum strontium manganite (LSMO) is the most widely used in industry because of its high curie temperature, photocatalytic activity, multiferroic properties, chemical phase stability, colossal magnetoresistance (CMR), magnetocaloric effect (MCE), structural stability, high electrical conductivity in an oxidizing atmosphere, thermal and small band gap energy [1-4]. The diverse physical properties of LSMO have irritated the interest of numerous nanotechnology-concerning applications like high-sensitivity and high-speed sensors of current and magnetic field, photooxidative reduction of organic wastes, non-volatile devices for recording and storing information, refrigerators, gas separation, energy production, new devices of the future for nonlinear optics, in microelectronics and spintronics [5-9]. For example, the effect of replacing some of the Mn with non-magnetic Ti^{4+} (d^0) on the structure, morphology and magnetic characteristics. In this context, the Ti^{4+} ionic radii (0.605A^0) has about the same ion of Mn^{3+} (0.645A^0) and are located between Mn4+ (0.530 Å) and Mn^{3+} (0.645 Å). The Mn^{4+} / Mn^{3+} ratio of the Mn framework, as well as the electrical and magnetic properties of manganites, depends on the substitution in the manganese sublattice. For proverb, the addition of Ti^{4+} minifies the number of Mn^{4+}-O^{2-}-Mn^{3+} networks as the result of the consistency of Ti^{4+}-O^{2-}-Mn^{3+} or Mn^{4+}-O^{2-}-Ti^{4+}. The reports of titanium-substituted manganite have shown a considerable decrease in Magnetic susceptibility, Specific magnetization, and the Curie temperature. For proverb, the addition of Ti^{4+} minifies the number of

*Corresponding author e-mail: hishamtash92@gmail.com.; (Hesham A. Hassan).

EJCHEM use only: Receive Date: 30 March 2022, Revise Date: 21 June 2022, Accept Date: 26 June 2022

DOI: 10.21608/ejchem.2022.130541.5752

Mn^{4+}-O^{2-}-Mn^{3+} networks as the result of the consistency of Ti^{4+}-O^{2-}-Mn^{3+} or Mn^{4+}-O^{2-}-Ti^{4+} [8, 10-15].

In this work, the impact of Ti^{4+} ion on the characterization of $La_{0.5}Sr_{0.5}Mn_{0.9}Ti_{0.1}O_3$ nanopowders elaborated using an organic acid precursor used glycine-nitrate as fuel was considered. The majority of prior works on manganite materials used solid-state reaction strategies. The advantages of the organic precursor pathway or sol-gel auto-combustion technology include the generation of nano-scale materials with a narrow size distribution, low agglomeration, simple processing, energy efficiency, and good homogeneity with regular microstructure [16]. Meanwhile, the manipulation of calcination temperature on the crystal structure, microstructure, and magnetic properties was also investigated. Finally, the antimicrobial and the anticancer properties were also investigated.

2. Experimental

2.1. Materials and Procedure

Table 1 exhibits stoichiometric amounts of pure chemicals with different weights for the synthesis of $La_{0.5}Sr_{0.5}Mn_{0.9}Ti_{0.1}O_3$. Starting chemicals; lanthanum nitrate hexahydrate $La(NO_3)_3.6H_2O$, anhydrous strontium nitrate $Sr(NO_3)_2$, manganese acetate tetrahydrate $Mn(CH_3COO)_2.4H_2O$ and titanium trichloride $TiCl_3$, were dissolved into distilled water. Then glycine was added as fuel. After that, the mixture was slowly heated on a hot plate magnetic stirrer at till evaporation occurred and viscous gel appeared. After auto combustion, LSMTO precursors are formed. Finally, the formed precursors were thermally heated at different temperatures from 800 to 1200°C for 2 h.

Table 1. Pure chemicals with different weights for the synthesis of LSMTO.

Chemicals used (g)	**Titanium ratio** 0.1
Lanthanum nitrate hexahydrate, $La(NO_3)_3.6H_2O$	2.5
Anhydrous strontium nitrate, $Sr(NO_3)_2$	1.22
Manganese acetate tetrahydrate, $C_4H_6MnO_4.4H_2O$	2.54
Titanium trichloride $TiCl_3$	0.17
Pure glycine NH_2CH_2COOH	3.53

2.2. Physical Characterization

Bruker AXS diffractometer (D8-ADVANCE Germany) with Cu Kα (λ = 1.54056 Å) radiation was recognized for X-ray powder diffraction (XRD) for LSMT. Field emission scanning electron microscopy was made by a FE-SEM (JEOL-JSM-5410 Japan). FT-IR electronic spectra were traced using a spectrometer (JASCO 3600) to note the vibrational modes of perovskite compounds. A Faraday balance is a device for measuring magnetic susceptibility. In this technique, the sample is suspended between electromagnet cores where a magnetic field is applied. Then, the sample is heated gradually using a non-inductive furnace. After measuring the pull of the balance (Δm), many parameters can be calculated such as the molar magnetic susceptibility (χm), and the molar magnetization (Mm) can be calculated using the following relations respectively:

$$\chi m=(\Delta m*g*Mw)/(m*H*(dH/dZ)) \quad (1)$$

$$Mm = \chi m* H \quad (2)$$

where: g is the gravity=980.6 cm s^{-2}, Mw is the molecular weight of the sample, m is the mass of the sample, H is the magnetizing field applied, dH/dZ is the magnetic field gradient in the z-direction[17].

3. Results and discussion

3.1 Crystal structure

Figure 1 shows XRD patterns of lanthanum strontium manganese titanium oxide (LSMTO) powders prepared by glycine nitrate process (GNP) with different calcination temperatures (800, 1000 and 1200 °C) for 2 h at 0.1 Ti ion content. Pure LSMTO single phase was obtained at (800, 1000, and 1200 °C). Obviously, diffraction peaks joined with the pure orthorhombic perovskite phase with space group Pbnm (ICDD card#l 01-082-8304) were matched. Peaks at 2θ values of 32.48°, 40.01°, 46.60°, 57.87°, 58.02°, and 68.02° of LSMTO was listed. The crystallite size of the $La_{0.5}Sr_{0.5}Mn_{0.9}Ti_{0.1}O_3$ show in table 2 according to Debye-Scherrer equation was increased with increasing calcination temperature.

Table 2. Crystallite size of $La_{0.5}Sr_{0.5}Mn_{0.9}Ti_{0.1}O_3$ at different calcination temperatures from 800 to 1200°C for 2 h.

Calcination temperature, °C	**Crystallite size nm**
800	13.57
1000	15.73
1200	16.10

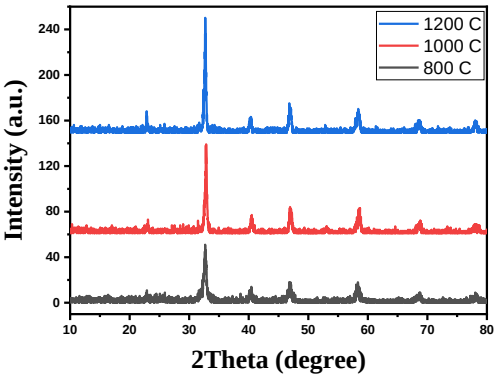

Fig. 1. The X-ray diffraction patterns of produced La0.5Sr0.5Mn0.9Ti0.1O3 prepared by glycine nitrate process (GNP) annealed at different calcinations temperature for 2 h.

3.2 FT-IR analysis

Figure 2 depicts FT-IR spectra of the produced $La_{0.5}Sr_{0.5}Mn_{0.9}Ti_{0.1}O_3$ powder annealed at different calcination temperatures (800, 1000, and 1200 °C) for 2 h in the range from 400 to 4000 cm^{-1}. Obviously, bands appeared at 565 cm^{-1} which can be assigned to the asymmetric and symmetric stretch of MnO_6 octahedra, the second peak was observed around 540 cm^{-1} due to Ti-O stretching mode, frequency band around 850 cm^{-1} due to Mn-O (metal-oxygen) stretching mode and is characteristic of the perovskite structure. The broadening of the stretching peak at 565 cm^{-1} with doping content Ti^{+4} may be induced due to the Mn–O and Ti–O stretching vibrations in Mn–O–Ti structure, representing that Ti is primarily in the tetravalent state [18-20]. The two absorption bands at 1454 cm^{-1} and 1617 cm^{-1} are associated with the C=O vibration and can be related to traces of carbonate. The peak between 1915-2112 cm^{-1}, was observed due to moisture content.

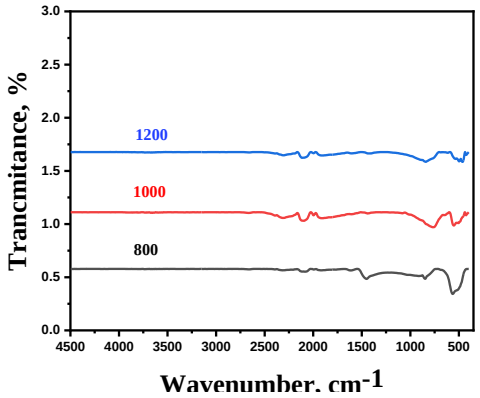

Fig. 2 The FT-IR spectrums of $La_{0.5}Sr_{0.5}Mn_{0.9}Ti_{0.1}O_3$ prepared by glycine nitrate process (GNP) process annealed at different calcinations temperature for 2 h.

3.3 Microstructure

3.3.1 FE-SEM investigation

Figure 3 (a, b, and c) display a representative field emission scanning electron micrographs (FE-SEM) of $La_{0.5}Sr_{0.5}Mn_{0.9}Ti_{0.1}O_3$ at different calcination temperatures (800, 1000, and 1200 °C) and calcinations time 2 h. The LSMTO was evinced as an irregular spherical structure at low temperature 800 ^{0}C and by increasing the annealing temperature the produced nanopowders were appeared as orthorhombic structure connected together to form clusters.

3.3.2 TEM Investigation

The transmission electron microscope TEM photograph of titanium substituted lanthanum strontium manganite $La_{0.5}Sr_{0.5}Mn_{0.9}Ti_{o.1}O_3$ prepared by GNP method at different calcination temperatures (800, 1000, and 1200 °C) for 2 h is illustrated in the Figure 4. At low decomposition temperature 800^{o}C, the products retain fluffy clustered polycrystalline nanopowders. Moreover, at high decomposition temperature, the optioned samples become more fluffy clustered polycrystalline nanopowders.

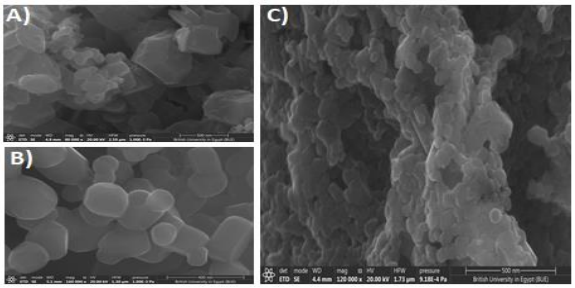

Fig. 3. FE-SEM micrographs of LSMTO prepared by the glycine nitrate process (GNP) at different calcination temperatures for 2 h: a) 800 °C, b) 1000 °C, and C) 1200 °C.

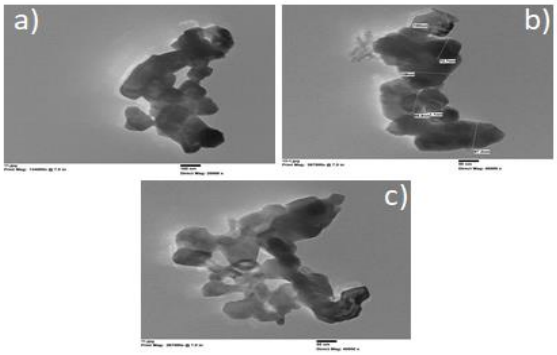

Fig. 4. TEM photograph of LSMT prepared by the GNP process at different calcination temperatures for 2 h: a) 800 °C, b) 1000 °C, and C) 1200 °C

3.4 Magnetic properties

The measurement of magnetic susceptibility is an interesting method for determining phase boundaries in magnetic systems. Temperature reliance of magnetization M(T) for $La_{0.5}Sr_{0.5}Mn_{0.9}Ti_{0.1}O_3$ synthesized through (GNP) method with different calcination temperatures (800, 1000, and 1200 °C) for 2 h is shown in Figure 5. Specific magnetization was measured under magnetic applied field (3225) Oe, the data expose the traditional trend of ferrimagnetic materials; with increasing the temperature the M(T) decreases to reach the paramagnetic region where the magnetocrystalline anisotropy ceases, and then magnetization drops at the well-known Curie point. The non-magnetic nature of Ti^{4+} (Ti^{4+} has electron configuration 3d0) cause of magnetic dilution. With partial substitution (10 %) of Ti^{+4} in the $La_{0.5}Sr_{0.5}Mn_{0.9}Ti_{0.1}O_3$ sample, Mn^{+3}-O-Mn^{+4} bonds replace with Mn^{+3}-O-Ti^{+4} bonds. Titanium substituted Mn-site straightway minifies the weakens the double-exchange interaction between Mn^{3+} and Ti^{4+} as a result of the default of double exchange [21, 22]. But super-exchange via oxygen 2p orbitals is improved when titanium substituted LSMTO. It suggests transfer metal-doped in Mn-site gives a negative contribution to DE mechanism. This phenomenon is a disturbance in

the long-order ferromagnetic arrangement on the network Mn–O–Mn [23-25]. Curie temperature value is specified by the minimum of dM/dT curve versus temperature and it is found to be 373, 373.32, and 383 K, respectively for $La_{0.5}Sr_{0.5}Mn_{0.9}Ti_{0.1}O_3$ calcined at different temperatures (800, 1000 and, 1200 °C)

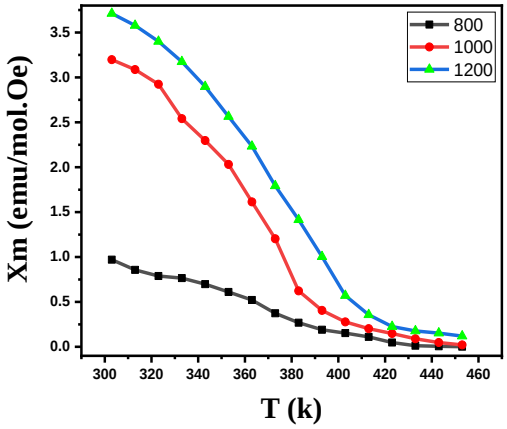

Fig. 5. Molar magnetic susceptibility (χm) vs. temperature of $La_{0.5}Sr_{0.5}Mn_{0.9}Ti_{0.1}O_3$ prepared by (GNP) process at different calcination temperatures (800, 100, 1200 °C) for 2 h.

3.5 Anti-microbial activity

$La_{0.5}Sr_{0.5}Mn_{0.9}Ti_{0.1}O_3$ nanopowders annealed at different calcination temperatures 800 , 1000 and 1200 °C were screened for their activities as antibacterial, against Gram positive of Staphylococcus aureus (ATCC25923), Bacillus subtilis (ATCC6635); Gram-negative species of Escherichia coli (ATCC 25922), Salm-onella typhimurium (ATCC 14028), Antimicrobial activity was tested by the disc diffusion method [26, 27]. Chloramphencol and Cephalothin were used as standard references for Gram-positive and Gram-negative bacteria. Data of the antibacterial of LSMT with different titanium ion contents were recorded in Table 3. The results involved different results as antimicrobial activity towards Gram-positive and Gram-negative was lower than the control.

3.6 Anticancer activity

Cell viability and cell inhibition (%) versus concentrations of $La_{0.5}Sr_{0.5}Mn_{0.9}Ti_{0.1}O_3$; LSMTO annealed at different temperatures 800, 1000, and 1200°C, respectively at concentrations from 0 to 500 µg/ml against the HepG-2 cell line is indicated in figure 6. The cell viability of HepG-2 decreased with augmented concentration of LSMTO nanoparticles significantly. At high concentrations of the samples, the anticancer effect results refer to the protuberance of the essential cell death. In this case, half-maximal inhibitory concentration IC_{50} was also registered for LSMTO samples calcined at different temperatures. For example, IC_{50} values 105, 135, and 152 µg/ml for LSMTO calcined at different temperatures 800, 1000, and 1200°C, respectively. The presented values ascribed to IC_{50} for the LSMTO samples is lower than nano CaO of 92.08 µg/mL [28] inhibits HepG-2 cell proliferation at about 50% (IC_{50}) after 48 h of treatment. The results can be discussed based on the particle size as well as the microstructures. Thereby, it is known that nanoparticle morphologies have a considerable impact on the cellular internalization. Sharp nanoparticle structures may introduce the membrane of endosome and localize to the cytoplasm [29-31].

Table 3 Antimicrobial result of LSMTO at different calcination temperature

	Gram-positive bacteria		**Gram-negative bacteria**	
LSMTO	Staphylococcus Aureus (ATCC 25923)	Bacillus subtilis (ATCC 6635)	Salmonella typhimurium (ATCC 14028)	Escherichia coli (ATCC 25922)
800 °C	12	12	11	10
1000 °C	8	8	10	10
1200 °C	10	7	9	8
Control	**35**	**35**	**36**	**38**

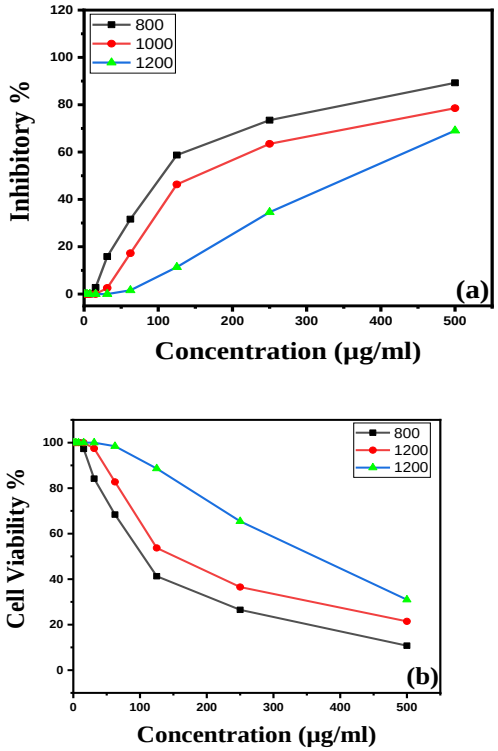

Figure7. (a) The cell viability and (b) cell inhibitory (%) versus concentrations of LSMTO calcination at different temperatures 800, 1000, and 1200°C at concentrations from 0 to 500 µg/m against HepG-2 cell line.

3.7 Conclusion

Lanthanum strontium titanium manganite nanopowders $La_{0.5}Sr_{0.5}Mn_{0.9}Ti_{0.1}O_3$; LSMTO at different temperatures was successfully fabricated using organic acid precursor strategy based on glycine nitrate GNP as a fuel. XRD diffraction profile depicted that the present LSMTO powders have orthorhombic structure. FT-IR spectrum illustrated the band peaks ascribed to perovskite orthorhombic structure. TEM images revealed that the present powders exhibited rhombohedral like structure. Molar magnetic susceptibility was notified to increase with the temperature. Subsequently, Curie temperature values were found to increase from 373 to 383 K with increasing the temperature, respectively. Antimicrobial activity of synthesized LSMTO powders towards Gram positive and Gram negative was examined and the results predicted that the efficacy of the formed powders were lower than the standard chloramphencol and cephalothin. Finally, LSMTO achieved the highest cytotoxic activity against HEP-G2 with IC_{50} value (105, 135 and 152 µg/ml) for $La_{0.5}Sr_{0.5}Mn_{0.9}Ti_{0.1}O_3$ calcined at different temperatures 800, 1000, and 1200 ^{0}C, respectively.

Acknowledgments

This research was supported by the Chemistry Department, Faculty of Science, Al-Azhar University Cairo. The authors would like their great appreciation to the technical services unit and the Electronic & Magnetic Materials Department, Advanced Materials Institute in Central Metallurgical Research and Development Institute (CMRDI) for their valuable and constructive suggestions during the experimental work and for characterization instruments of this research work.

.

Reference

1. Žužić A, Ressler A, Macan J: **Evaluation of carbonate precursors in manganite coprecipitation synthesis by Fourier transform infrared (FTIR) spectroscopy.** *Solid State Communications* 2022, **341:**114594.
2. Pchelina D, Sedykh V, Chistyakova N, Rusakov V, Alekhina Y, Tselebrovskiy A, Fraisse B, Stievano L, Sougrati MT: **Alkaline-earth metal-doped perovskites La0. 95A0. 05MnO3+ δ (A= Ca, Sr): New structural and magnetic features revealed by 57Fe Mössbauer spectroscopy and magnetic measurements.** *Journal of Physics Chemistry of Solids* 2021, **159:**110268.
3. Im J, Park I, Shin D: **Electrochemical properties of nanostructured lanthanum strontium manganite cathode fabricated by electrostatic spray deposition.** *Solid State Ionics* 2011, **192:**448-452.
4. Zhang J, Huang W, Hu T, Wang Y: **Effect of organic additions on crystal growth behavior of La0. 8Sr0. 2MnO3 nanopowders prepared via sol–gel process.** *Journal of Crystal Growth* 2021, **571:**126253.
5. Wei Z, Pashchenko A, Liedienov N, Zatovsky I, Butenko D, Li Q, Fesych I, Turchenko V, Zubov E, Polynchuk PY: **Multifunctionality of lanthanum–strontium manganite nanopowder.** *Physical Chemistry Chemical Physics* 2020, **22:**11817-11828.
6. Turky AO, Rashad MM, Hassan AM, Elnaggar EM, Bechelany M: **Optical, electrical and magnetic properties of lanthanum strontium manganite La 1− x Sr x MnO 3 synthesized through the citrate combustion method.** *Physical Chemistry Chemical Physics* 2017, **19:**6878-6886.
7. Turky AO, Rashad MM, Hassan AM, Elnaggar EM, Zhao H, Bechelany M: **Tunable investigation optical, electrical and magnetic behaviors of Gd3+ substituted lanthanum strontium manganite La0. 5-x Sr0. 5GdxMnO3 nanopowders facilely synthesized through citrate precursor technique.** *Journal of Alloys Compounds* 2018, **735:**2175-2181.
8. Estemirova SK, Mitrofanov VY, Uporov S, Gulyaeva R: **Effect of cation substitution on structural, magnetic and magnetocaloric properties of (La0. 7Eu0. 3) 0.75 Sr0. 25Mn0. 9 (Me) 0.1 O3 (Me= Co, Ti).** *Journal of Magnetism Magnetic Materials* 2020, **502:**166593.
9. Hosseininejad S, Ehsani M, Esmaeili SJ: **Structural and magnetic properties of yttrium-substituted La 0.6-xYxSr0. 4MnO3 (x= 0–0.3).** *Ceramics International* 2021, **47:**11536-11546.
10. Kim M, Yang J, Cai Q, Zhou X, James WJ, Yelon WB, Parris PE, Buddhikot D, Malik SK: **Structure, magnetic, and transport properties of Ti-substituted La 0.7 Sr 0.3 MnO 3.** *Physical Review B* 2005, **71:**014433.
11. Yanchevskiĭ O, V'yunov O, Belous A, Tovstolytkin A, Kravchik V: **Synthesis and characterization of La0. 7Sr0. 3Mn1− x TixO3 manganites.** *Physics of the Solid State* 2006, **48:**709-716.
12. Kumar D, Singh AK: **Investigation of structural and magnetic properties of Nd0. 7Ba0. 3Mn1-xTixO3 (x= 0.05, 0.15 and 0.25) manganites synthesized through a single-step process.** *Journal of Magnetism Magnetic Materials* 2019, **469:**264-273.
13. Jadav G, Kanjariya P, Chavda S, Bhalodia J: **Effect of Al and Ti substitution on the structural and magnetotransport properties of Lanthanum-Strontium manganite.** In *AIP Conference Proceedings*. AIP Publishing LLC; 2018: 020002.

14. Phong P, Bau L, Hoan L, Manh D, Phuc N, Lee I-JJ: **Effect of B-site Ti doping on the magnetic, low–field magnetocaloric and electrical transport properties of La0. 7Sr0. 3Mn1− xTixO3 perovskites.** *Journal of Alloys Compounds* 2016, **656:**920-928.
15. Estemirova SK, Mitrofanov VY, Uporov S, Gulyaeva RJ: **Effect of cation substitution on structural, magnetic and magnetocaloric properties of (La0. 7Eu0. 3) 0.75 Sr0. 25Mn0. 9 (Me) 0.1 O3 (Me= Co, Ti).** *Journal of Magnetism Magnetic Materials* 2020, **502:**166593.
16. Turky AO, Rashad MM, Zaki ZI, Ibrahim IA, Bechelany M: **Tuning the optical and dielectric properties of calcium copper titanate Ca x Cu 3− x Ti 4 O 12 nanopowders.** *RSC Advances* 2015, **5:**18767-18772.
17. Roumaih K: **Effect of temperature on the dielectric and magnetic properties of NiFe2O4@ MgFe2O4 and ZnFe2O4@ MgFe2O4 core-shell.** *Physica Scripta* 2021, **96:**125809.
18. Afify MS, El Faham MM, Eldemerdash U, El Rouby WM, El-Dek S: **Room temperature ferromagnetism in Ag doped LaMnO3 nanoparticles.** *Journal of Alloys Compounds* 2021, **861:**158570.
19. Gholamrezaei S, Amiri M, Amiri O, Salavati-Niasari M, Moayedi H: **Ultrasound-accelerated synthesis of uniform SrMnO3 nanoparticles as water-oxidizing catalysts for water splitting systems.** *Ultrasonics sonochemistry* 2020, **62:**104899.
20. Priolkar K, Rawat R: **Effect of heterovalent substitution at Mn site on the magnetic and transport properties of La0. 67Sr0. 33MnO3.** *Journal of magnetism magnetic materials* 2008, **320:**325-330.
21. Kallel N, Ihzaz N, Kallel S, Hagaza A, Oumezzine M: **Research on charge-ordering state in La0. 5Sr0. 5MnO2. 88 and La0. 5Sr0. 5Mn0. 5Ti0. 5O3 systems.** *Journal of Magnetism Magnetic Materials* 2009, **321:**2285-2289.
22. Millis A: **Lattice effects in magnetoresistive manganese perovskites.** *Nature* 1998, **392:**147-150.
23. Kallel N, Dezanneau G, Dhahri J, Oumezzine M, Vincent H: **Structure, magnetic and electrical behaviour of La0. 7Sr0. 3Mn1− xTixO3 with 0⩽ x⩽ 0.3.** *Journal of Magnetism Magnetic Materials* 2003, **261:**56-65.
24. Nam D, Bau L, Khiem N, Dai N, Hong L, Phuc N, Newrock R, Nordblad P: **Selective dilution and magnetic properties of La 0.7 Sr 0.3 Mn 1− x M x′ O 3 (M′= Al, Ti).** *Physical Review B* 2006, **73:**184430.
25. Dayal V, Kumar V P, Hadimani RL, Jiles DC: **Evolution of Griffith's phase in La0. 4Bi0. 6Mn1− xTixO3 perovskite oxide.** *Journal of Applied Physics* 2014, **115:**17E111.
26. Bauer A: **Antibiotic susceptibility testing by a standardized single disc method.** *Am J clin pathol* 1966, **45:**149-158.
27. Barry AL: **An overview of the Clinical and Laboratory Standards Institute (CLSI) and its impact on antimicrobial susceptibility tests.** *Antimicrobial susceptibility testing protocols* 2007**:**1-6.
28. Yoonus J, Resmi R, Beena B: **Greener nanoscience: Piper betel leaf extract mediated synthesis of CaO nanoparticles and evaluation of its antibacterial and anticancer activity.** *Materials Today: Proceedings* 2021, **41:**535-540.
29. Ahmadian E, Dizaj SM, Rahimpour E, Hasanzadeh A, Eftekhari A, Halajzadeh J, Ahmadian H: **Effect of silver nanoparticles in the induction of apoptosis on human hepatocellular carcinoma (HepG2) cell line.** *Materials Science Engineering: C* 2018, **93:**465-471.
30. Thai SF, Wallace KA, Jones CP, Ren H, Grulke E, Castellon BT, Crooks J, Kitchin KT: **Differential genomic effects of six different TiO2 nanomaterials on human liver HepG2 cells.** *Journal of biochemical molecular toxicology* 2016, **30:**331-341.
31. Turky AO, Abdelmoaz MA, Hessien MM, Hassan AM, Bechelany M, Ewais EM, Rashad MM: **A Robust and Highly Precise Alternative against the Proliferation of Intestinal Carcinoma and Human Hepatocellular Carcinoma Cells Based on Lanthanum Strontium Manganite Nanoparticles.** *Materials* 2021, **14:**4979.